Higher order hierarchical H(curl) Legendre basis functions applied in the finite element method: emphasis on microwave circuits

Johannesson, Peter

2011

CODEN:LUTEDX/(TEAT-7205)/1-11/(2011)

Higher order hierarchical *H*(curl) Legendre basis functions applied in the finite element method: emphasis on microwave circuits

Peter Johannesson

Electromagnetic Theory
Department of Electrical and Information Technology
Lund University
Sweden

Peter Johannesson
Peter.Johannesson@eit.lth.se

Department of Electrical and Information Technology
Electromagnetic Theory
Lund University
P.O. Box 118
SE-221 00 Lund
Sweden

Editor: Gerhard Kristensson

Abstract

In this paper a set of higher order hierarchical $H(\mathrm{curl})$ Legendre basis functions is introduced as a basis in the two and three dimensional finite element method (FEM). The basis functions are divided into three different sets: edge functions, surface functions and interior functions. Two problems are addressed in order to study the p-convergence of the representation. In the first problem the eigenvalues of an inhomogeneous rectangular waveguide with a rectangular inclusion are computed. The p-convergence is measured for a dielectric inclusion and for an inclusion with finite conductivity, respectively. In the second problem the eigenvalues of a homogeneous cubic cavity are computed in order to measure the p-convergence for the three dimensional representation.

1 Introduction

In RF electronics there is a desire to simulate wire based structures, *e.g.*, transmission lines, inductors, baluns and transformers. The goal is often to achieve the circuite parameters of the equivalent circuite model, *i.e.*, the lumped model, of the structure. The lumped model can thereafter be used in the circuite design tool in order to increase the accuracy of the total design. Since there is a request of high accuracy, the finite element method (FEM) is often used to compute the different quantities. A problem with this approach is that three dimensional problems are computational demanding and the number of degrees of freedom (DOF) is, in general, very large. This is mainly due to two factors: the large surrounding space that must be inserted around the geometry of interest in order to model the free space, and the mathematical representation, *i.e.*, the basis functions. The part caused by the first factor can be reduced if a proper boundary condition can be applied or avoided if the FEM can be combined with the method of moment (MoM) in a hybrid FEM/MoM formulation. The part caused by the second factor can, for some problems, be reduced if a more suitable representation is applied. The by far most common representation used in the FEM is the Whitney I elements [2] (also known as the edge elements). Since these are based on polynomials of first order the convergence rate is rather slow. For some problems the convergence rate can be increased by increasing the polynomial order of the basis. Two different forms exist: higher order interpolatory basis functions [3] and higher order hierarchical basis functions [11]. An advantage of the hierarchical basis functions is that the polynomial order of the basis functions does not have to be kept constant over the whole mesh which conveys a more flexible property compared to the interpolatory basis functions.

In order to improve the representation, and thereby reduce the number of DOF, for the geometry in question, *i.e.*, the wire based structures, it is desirable to use large cells including hierarchical basis functions. Due to the shape of the wires on integrated circuits, *i.e.*, a rectangular cross section, it might be possible to reduce the number of DOF if hexahedral cells [1] are chosen instead of the common tetrahedral cells. In [5] a set of higher order hierarchical $H(\mathrm{div})$ basis functions for quadrilateral cells was introduced. Due to the relation between the $H(\mathrm{curl})$ and $H(\mathrm{div})$ function

spaces it is possible to achieve a set of higher order hierarchical $H(\mathrm{curl})$ basis functions for quadrilateral surface cells. Generalizing this representation yields a basis defined on hexahedral volume cells.

A problem with higher order basis functions is that the advantages are lost when the fields contain singularities. For a waveguide structure, including smooth fields, $\mathcal{O}h^{2p}$ errors are obtained when scattering parameters are computed on meshes with uniform h and p [4]. The parameter h corresponds to the element size and p is the order number of the polynomial of the basis functions. For solutions containing singularities the p dependence is lost and instead $\mathcal{O}h^{2\alpha}$ errors are obtained. The parameter $\alpha < 1$ is dependent on the singularity, only. For Laplacian problems the convergence can be estimated to fulfill [8, 10]

$$\|u - u_p\|_m \leq Ch^{\mu} \|u\|_r$$

where $\mu = \min(p + 1 - m, r - m)$ is the rate of the convergence. The regularity of the solution and the order of the derivation are denoted by r and m, respectively. If singularities are present $r - m$ can become smaller than $p + 1 - m$ which conveys that μ is independent of p. For high frequencies and large objects, *i.e.*, when the extension of the cross sectional surface is much larger than the skin depth, the p-dependency is negligible and the convergence rate is in principle only dependent on h. It is therefore of interest to investigate the efficiency of higher order basis functions at different rates between the skin depth and the extension of the cross-sectional surface and at what point the p-dependency of the convergence is lost.

The representation will be examined for two different geometries: a cubic homogeneous cavity and a rectangular waveguide, including an inclusion with a complex valued permittivity. In order to investigate how the convergence of the method is affected by the permittivity of the inclusion, two different studies are performed. One in which the real part of the permittivity is varied and the imaginary part is zero, and one in which the real part is kept constant and the imaginary part is varied. The second study corresponds to the case when the inclusions are conductive.

2 Basis functions

The $H(\mathrm{curl};\Omega)$ basis functions that are applied in this paper are based on the $H(\mathrm{div};\Omega)$ basis functions that initially were introduced in [5]. The $H(\mathrm{curl};\Omega)$ basis functions are defined on parameterized quadrilateral cells where each cell is spanned by the local parametric (u, v) coordinate system defined by $-1 \leq u, v \leq 1$. The $H(\mathrm{curl};\Omega)$ and $H(\mathrm{div};\Omega)$ function spaces are defined as

$$\begin{aligned} H(\mathrm{curl};\Omega) =& \{\boldsymbol{u} : \langle \boldsymbol{u}, \boldsymbol{u} \rangle_\Omega < \infty, \langle \nabla \times \boldsymbol{u}, \nabla \times \boldsymbol{u} \rangle_\Omega < \infty\}, \\ H(\mathrm{div};\Omega) =& \{\boldsymbol{u} : \langle \boldsymbol{u}, \boldsymbol{u} \rangle_\Omega < \infty, \langle \nabla \cdot \boldsymbol{u}, \nabla \cdot \boldsymbol{u} \rangle_\Omega < \infty\}. \end{aligned}$$

For two dimensional problems the basis functions are developed to span the fields in quadrilateral cells [6]. The representation reads

$$\boldsymbol{a}^u H_u^{mn}(u, v), \quad \boldsymbol{a}^v H_v^{mn}(u, v), \quad m, n = 0, 1, \ldots,$$

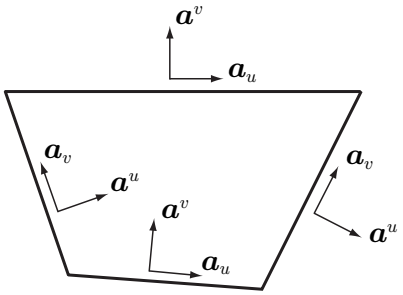

Figure 1: A quadrilateral cell including the covariant and contravariant unitary vectors at different positions.

where

$$\boldsymbol{a}^u = \nabla u, \quad \boldsymbol{a}^v = \nabla v,$$

are the contravariant unitary vectors [9]. These are related to the covariant unitary vectors,

$$\boldsymbol{a}_u = \frac{\partial \boldsymbol{r}}{\partial u}, \quad \boldsymbol{a}_v = \frac{\partial \boldsymbol{r}}{\partial v},$$

and fulfill $\boldsymbol{a}^i \cdot \boldsymbol{a}_j = \delta_{ij}$ as is illustrated in Figure 1. The functions H_ℓ^{mn} are defined as

$$\begin{cases} H_u^{mn}(u,v) = \widetilde{C}_m \widetilde{P}_m(v) C_n P_n(u), \\ H_v^{mn}(u,v) = \widetilde{C}_m \widetilde{P}_m(u) C_n P_n(v) \end{cases}$$

where P_n are the Legendre polynomials. The functions $\widetilde{P}_m(\cdot)$ are defined as

$$\widetilde{P}_m(\cdot) = \begin{cases} 1 - (\cdot), & m = 0, \\ 1 + (\cdot), & m = 1, \\ P_m(\cdot) - P_{m-2}(\cdot), & m \geq 2, \end{cases}$$

and the coefficients as

$$\widetilde{C}_m = \begin{cases} \frac{\sqrt{3}}{4}, & m = 0, 1, \\ \frac{1}{2}\sqrt{\frac{(2m-3)(2m+1)}{2m-1}}, & m \geq 2, \end{cases}$$

$$C_n = \sqrt{n + \frac{1}{2}}.$$

To fulfill the Nedelec constraint [7] the order numbers must be chosen in accordance to $N_u = M_u - 1$ and $N_v = M_v - 1$. This means that the order of the derivated part should be the same as the other part. The stated values are upper limits for the order numbers of the derivated part which means that larger values do not contribute to a higher accuracy of the solution. Lower values of the order number can of course be chosen with a decrease in the accuracy as a consequence. Note that the lowest order functions, *i.e.*, $M_u = M_v = 1, N_u = N_v = 0$, correspond to the Whitney I basis functions [2].

For three dimensional problems the basis functions are developed to span the fields in hexahedral cells [1]. The representation yields

$$\boldsymbol{a}^u H_u^{kmn}(u,v,w), \quad \boldsymbol{a}^v H_v^{kmn}(u,v,w), \quad \boldsymbol{a}^w H_w^{kmn}(u,v,w), \quad k,m,n = 0,1,\ldots$$

where

$$\begin{cases} H_u^{kmn}(u,v,w) = \widetilde{C}_k \widetilde{P}_k(v) \widetilde{C}_m \widetilde{P}_m(w) C_n P_n(u), \\ H_v^{kmn}(u,v,w) = \widetilde{C}_k \widetilde{P}_k(w) \widetilde{C}_m \widetilde{P}_m(u) C_n P_n(v), \\ H_w^{kmn}(u,v,w) = \widetilde{C}_k \widetilde{P}_k(u) \widetilde{C}_m \widetilde{P}_m(v) C_n P_n(w). \end{cases} \tag{2.1}$$

The basis functions can be divided into three classes: edge functions, surface functions and interior functions. The edge functions are represented by

$$\boldsymbol{a}^\ell H_\ell^{00n}, \quad \boldsymbol{a}^\ell H_\ell^{01n}, \quad \boldsymbol{a}^\ell H_\ell^{10n}, \quad \boldsymbol{a}^\ell H_\ell^{11n}, \quad \ell \in \{u,v,w\}, \quad n \geq 0,$$

the surface functions are represented by

$$\boldsymbol{a}^\ell H_\ell^{k0n}, \quad \boldsymbol{a}^\ell H_\ell^{k1n}, \quad \boldsymbol{a}^\ell H_\ell^{0mn}, \quad \boldsymbol{a}^\ell H_\ell^{1mn}, \quad \ell \in \{u,v,w\}, \quad k,m \geq 2, \quad n \geq 0,$$

and the interior functions are represented by

$$\boldsymbol{a}^\ell H_\ell^{kmn}, \quad \ell \in \{u,v,w\}, \quad k,m \geq 2, \quad n \geq 0.$$

The general properties of the three classes of functions are that they all reach there maximum value at some part in the cell and vanishes at other parts. For the edge functions the tangential component, *e.g.*, $\boldsymbol{a}_\ell \cdot \boldsymbol{a}^\ell H_\ell^{00n}$, is maximal at one edge and vanishes on the other edges (see Figure 1). The tangential component of the surface function, *e.g.*, $\boldsymbol{a}_\ell \cdot \boldsymbol{a}^\ell H_\ell^{k0n}$, reaches its maximum value on one surface and vanishes on the edges of the cell. The tangential component of the interior function, *e.g.*, $\boldsymbol{a}_\ell \cdot \boldsymbol{a}^\ell H_\ell^{kmn}$, vanishes on the boundary of the cell, *i.e.*, it vanishes on the edges and the surfaces of the cell. From the properties of the edge, the surface and the interior functions we find that that continuity of the electric and magnetic fields, between adjacent cells, are preserved by the edge functions and the surface functions whereas the interior functions only are used to span the fields on the inside of the respective cell and do not couple to the adjacent cells. This is valid for three dimensional problems. For two dimensional problems the fields are spanned by the edge and the surface functions. In this case it is only the edge functions that secure that the continuity of the fields, between adjacent cells, are preserved whereas the surface functions are used to span the fields inside the respective cell. This means that the surface functions work as interior functions for two dimensional problems.

3 FEM formulation

3.1 Inhomogeneous waveguide

For two dimensional inhomogeneous electric media $E_z = 0$ can not be assumed. This means that all three components of the electric field must be included in the

calculations even if the problem is regarded as two dimensional. For the waveguide the electric field is assumed to fulfill

$$\boldsymbol{E}(\boldsymbol{r}) = \boldsymbol{E}(\boldsymbol{\rho})\mathrm{e}^{-\gamma z}, \quad \boldsymbol{\rho} \in \Omega,$$

where $\gamma = \alpha + \mathrm{j}\beta$ is the propagating constant and Ω is the cross sectional surface of the waveguide. The time convention $\boldsymbol{E}(\boldsymbol{r}, \omega) = \boldsymbol{E}(\boldsymbol{r})\mathrm{e}^{\mathrm{j}\omega t}$ is assumed. Insertion into the Maxwell's equations

$$\nabla \times \boldsymbol{E} = -\mathrm{j}\omega\mu\boldsymbol{H} = -\mathrm{j}\omega\mu_0\mu_\mathrm{c}\boldsymbol{H}, \tag{3.1}$$
$$\nabla \times \boldsymbol{H} = (\sigma + \mathrm{j}\omega\epsilon)\boldsymbol{E} = \mathrm{j}\omega\epsilon_0\epsilon_\mathrm{c}\boldsymbol{E}. \tag{3.2}$$

leads to the three component form

$$\nabla_\mathrm{t} \times \frac{1}{\mu_\mathrm{c}}\nabla_\mathrm{t} \times \boldsymbol{E}_\mathrm{t} - \gamma\frac{1}{\mu_\mathrm{c}}(\nabla_\mathrm{t} E_z + \gamma\boldsymbol{E}_\mathrm{t}) = k_0^2\epsilon_\mathrm{c}\boldsymbol{E}_\mathrm{t}, \tag{3.3}$$
$$\nabla_\mathrm{t} \times \left[\frac{1}{\mu_\mathrm{c}}(\nabla_\mathrm{t} E_z + \gamma\boldsymbol{E}_\mathrm{t}) \times \hat{\boldsymbol{z}}\right] = k_0^2\epsilon_\mathrm{c}\hat{\boldsymbol{z}}E_z. \tag{3.4}$$

Introduce

$$\begin{cases} \boldsymbol{e}_\mathrm{t} = \gamma\boldsymbol{E}_\mathrm{t}, \\ e_z = E_z. \end{cases}$$

Insertion into (3.3) and (3.4) yields

$$\begin{aligned} &\nabla_\mathrm{t} \times \frac{1}{\mu_\mathrm{c}}\nabla_\mathrm{t} \times \boldsymbol{e}_\mathrm{t} - \gamma^2\frac{1}{\mu_\mathrm{c}}(\nabla_\mathrm{t} e_z + \boldsymbol{e}_\mathrm{t}) = k_0^2\epsilon_\mathrm{c}\boldsymbol{e}_\mathrm{t}, \\ &\gamma^2\nabla_\mathrm{t} \times \left[\frac{1}{\mu_\mathrm{c}}(\nabla_\mathrm{t} e_z + \boldsymbol{e}_\mathrm{t}) \times \hat{\boldsymbol{z}}\right] = \gamma^2 k_0^2\epsilon_\mathrm{c}\hat{\boldsymbol{z}}e_z. \end{aligned} \tag{3.5}$$

The weak solution of (3.5) is a complex number γ and a function $\boldsymbol{e} = \boldsymbol{e}_\mathrm{t} + \hat{\boldsymbol{z}}e_z$ for which the bilinear functional

$$\begin{aligned} B(\boldsymbol{w}, \boldsymbol{e}) = &-\int_\Omega \boldsymbol{w} \cdot \left(\nabla_\mathrm{t} \times \frac{1}{\mu_\mathrm{c}}\nabla_\mathrm{t} \times \boldsymbol{e}_\mathrm{t}\right) \mathrm{d}\Omega + \gamma^2 \int_\Omega \frac{1}{\mu_\mathrm{c}}\boldsymbol{w} \cdot (\nabla_\mathrm{t} e_z + \boldsymbol{e}_\mathrm{t}) \,\mathrm{d}\Omega \\ &+ \gamma^2 \int_\Omega \boldsymbol{w} \cdot \left\{\nabla_\mathrm{t} \times \left[\frac{1}{\mu_\mathrm{c}}(\nabla_\mathrm{t} e_z + \boldsymbol{e}_\mathrm{t}) \times \hat{\boldsymbol{z}}\right]\right\} \mathrm{d}\Omega \\ &+ k_0^2 \int_\Omega \epsilon_\mathrm{c}\boldsymbol{w} \cdot \boldsymbol{e}_\mathrm{t} \,\mathrm{d}\Omega - \gamma^2 k_0^2 \int_\Omega \epsilon_\mathrm{c}\boldsymbol{w} \cdot \hat{\boldsymbol{z}}e_z \,\mathrm{d}\Omega = 0, \quad \boldsymbol{w}, \boldsymbol{e} \in U(\Omega). \end{aligned} \tag{3.6}$$

The admissible function space is defined as

$$U(\Omega) = \left\{\boldsymbol{v} \in H(\mathrm{curl}; \Omega) : \hat{\boldsymbol{z}} \cdot (\nabla_\mathrm{t} \times \boldsymbol{v}_\mathrm{t}) \in L^2(\Omega), \nabla_\mathrm{t} v_z \in \{L^2(\Omega)\}^2, \boldsymbol{v} \in \{L^2(\Omega)\}^3\right\}$$

where L^2 is the set of square-integrable functions in the domain Ω. Applying the boundary conditions $\hat{\boldsymbol{n}} \times \boldsymbol{e}_\mathrm{t} = \boldsymbol{0}$ and $e_z = 0$ the bilinear functional becomes

$$\begin{aligned} B(\boldsymbol{w}, \boldsymbol{e}) = &\gamma^2 \int_\Omega \frac{1}{\mu_\mathrm{c}}(\nabla_\mathrm{t} w_z + \boldsymbol{w}_\mathrm{t}) \cdot (\nabla_\mathrm{t} e_z + \boldsymbol{e}_\mathrm{t}) \,\mathrm{d}\Omega - \gamma^2 k_0^2 \int_\Omega \epsilon_\mathrm{c} w_z e_z \,\mathrm{d}\Omega \\ &- \int_\Omega \frac{1}{\mu_\mathrm{c}}(\nabla_\mathrm{t} \times \boldsymbol{e}_\mathrm{t}) \cdot (\nabla_\mathrm{t} \times \boldsymbol{w}_\mathrm{t}) \,\mathrm{d}\Omega + k_0^2 \int_\Omega \epsilon_\mathrm{c}\boldsymbol{w}_\mathrm{t} \cdot \boldsymbol{e}_\mathrm{t} \,\mathrm{d}\Omega = 0 \end{aligned} \tag{3.7}$$

which leads to the equation

$$\begin{aligned}
&\int_\Omega \frac{1}{\mu_\mathrm{c}}(\nabla_\mathrm{t}\times\boldsymbol{w}_\mathrm{t})\cdot(\nabla_\mathrm{t}\times\boldsymbol{e}_\mathrm{t})\,\mathrm{d}\Omega - k_0^2\int_\Omega \epsilon_\mathrm{c}\boldsymbol{w}_\mathrm{t}\cdot\boldsymbol{e}_\mathrm{t}\,\mathrm{d}\Omega\\
&=\gamma^2\Big\{\int_\Omega \frac{1}{\mu_\mathrm{c}}\nabla_\mathrm{t}w_z\cdot\nabla_\mathrm{t}e_z\,\mathrm{d}\Omega+\int_\Omega\frac{1}{\mu_\mathrm{c}}\boldsymbol{w}_\mathrm{t}\cdot\nabla_\mathrm{t}e_z\,\mathrm{d}\Omega\\
&\quad+\int_\Omega\frac{1}{\mu_\mathrm{c}}\nabla_\mathrm{t}w_z\cdot\boldsymbol{e}_\mathrm{t}\,\mathrm{d}\Omega+\int_\Omega\frac{1}{\mu_\mathrm{c}}\boldsymbol{w}_\mathrm{t}\cdot\boldsymbol{e}_\mathrm{t}\,\mathrm{d}\Omega-k_0^2\int_\Omega\epsilon_\mathrm{c}w_ze_z\,\mathrm{d}\Omega\Big\}.
\end{aligned}$$

The subspace used in the current finite element (FE) implementation is

$$U^f=\left\{\boldsymbol{v}\in H(\mathrm{curl};\Omega):\boldsymbol{v}_\mathrm{t}=\boldsymbol{a}^\ell H_\ell^{mn}, v_z=(\hat{\boldsymbol{z}}\cdot\boldsymbol{a}^w)H_w^{mn},\ \ell\in\{u,v\},\ m,n\in\mathbb{Z}^+\right\}.$$

The expansion of the function $\boldsymbol{e}$ yields

$$\begin{aligned}
\boldsymbol{e}_\mathrm{t}(\boldsymbol{r})=&\boldsymbol{a}^u\sum_{k=0}^{K_v}\sum_{n=0}^{N_u}b_u^{kn}H_u^{kn}(u,v)+\boldsymbol{a}^v\sum_{m=0}^{M_u}\sum_{n=0}^{N_v}b_v^{mn}H_v^{mn}(u,v),\\
e_z(\boldsymbol{r})=&(\hat{\boldsymbol{z}}\cdot\boldsymbol{a}^w)\sum_{k=0}^{K_u}\sum_{m=0}^{M_v}b_w^{km}H_w^{km}(u,v)
\end{aligned}$$

By setting $B(\boldsymbol{w},\boldsymbol{e})=0$, for every $\boldsymbol{w},\boldsymbol{e}\in U^f$, we achieve the finite dimensional representation of the problem

$$\begin{pmatrix}\frac{1}{\mu_\mathrm{c}}\mathbf{S}_\mathrm{t}-k_0^2\epsilon_\mathrm{c}\mathbf{T}_\mathrm{t} & \mathbf{0}\\ \mathbf{0} & \mathbf{0}\end{pmatrix}\begin{pmatrix}\mathbf{b}_\mathrm{t}\\ \mathbf{b}_z\end{pmatrix}=\gamma^2\begin{pmatrix}\frac{1}{\mu_\mathrm{c}}\mathbf{T}_\mathrm{t} & \frac{1}{\mu_\mathrm{c}}\mathbf{G}\\ \frac{1}{\mu_\mathrm{c}}\mathbf{G}^\mathrm{T} & \frac{1}{\mu_\mathrm{c}}\mathbf{S}_z-k_0^2\epsilon_\mathrm{c}\mathbf{T}_z\end{pmatrix}\begin{pmatrix}\mathbf{b}_\mathrm{t}\\ \mathbf{b}_z\end{pmatrix}. \tag{3.8}$$

The elements of the matrices are

$$\begin{aligned}
&[\mathbf{S}_\mathrm{t}]_{e\ell'm'n'\ell mn}=\langle\nabla_\mathrm{t}\times\boldsymbol{a}^{\ell'}H_{\ell'}^{m'n'},\nabla_\mathrm{t}\times\boldsymbol{a}^\ell H_\ell^{mn}\rangle_{\Omega_e}, && [\mathbf{T}_\mathrm{t}]_{e\ell'm'n'\ell mn}=\langle\boldsymbol{a}^{\ell'}H_{\ell'}^{m'n'},\boldsymbol{a}^\ell H_\ell^{mn}\rangle_{\Omega_e},\\
&[\mathbf{G}]_{e\ell'm'n'mn}=\langle\boldsymbol{a}^{\ell'}H_{\ell'}^{m'n'},\nabla_\mathrm{t}(\hat{\boldsymbol{z}}\cdot\boldsymbol{a}^w)H_w^{mn}\rangle_{\Omega_e}, && [\mathbf{G}]^\mathrm{T}_{em'n'\ell mn}=\langle\nabla_\mathrm{t}(\hat{\boldsymbol{z}}\cdot\boldsymbol{a}^w)H_w^{m'n'},\boldsymbol{a}^\ell H_\ell^{mn}\rangle_{\Omega_e},\\
&[\mathbf{S}_z]_{em'n'mn}=\langle\nabla_\mathrm{t}(\hat{\boldsymbol{z}}\cdot\boldsymbol{a}^w)H_w^{m'n'},\nabla_\mathrm{t}(\hat{\boldsymbol{z}}\cdot\boldsymbol{a}^w)H_w^{mn}\rangle_{\Omega_e}, && [\mathbf{T}_z]_{em'n'mn}=\langle(\hat{\boldsymbol{z}}\cdot\boldsymbol{a}^w)H_w^{m'n'},(\hat{\boldsymbol{z}}\cdot\boldsymbol{a}^w)H_w^{mn}\rangle_{\Omega_e}
\end{aligned}$$

where $\ell',\ell\in\{u,v\}$ and Ω_e is the domain of cell e.

3.2 Resonance cavity

Let Ω be the interior domain of the cavity. From (3.1) and (3.2) we get the Helmholtz equation for the three dimensional problem

$$\nabla\times\frac{1}{\mu_\mathrm{c}}\nabla\times\boldsymbol{E}-k_0^2\epsilon_\mathrm{c}\boldsymbol{E}=\mathbf{0}. \tag{3.9}$$

Introduce a symmetric, bilinear functional

$$B(\boldsymbol{w},\boldsymbol{E})=\int_\Omega\boldsymbol{w}\cdot(\nabla\times\frac{1}{\mu_\mathrm{c}}\nabla\times\boldsymbol{E})\,\mathrm{d}\Omega-k_0^2\int_\Omega\boldsymbol{w}\cdot\epsilon_\mathrm{c}\boldsymbol{E}\,\mathrm{d}\Omega$$

where $\boldsymbol{w} \in H(\mathrm{curl};\Omega)$ is a proper weight function. Partial integration and applying the PEC boundary condition yield

$$B(\boldsymbol{w},\boldsymbol{E}) = \langle \nabla\times\boldsymbol{w}, \frac{1}{\mu_\mathrm{c}}\nabla\times\boldsymbol{E}\rangle_\Omega - \langle \boldsymbol{w}, k_0^2\epsilon_\mathrm{c}\boldsymbol{E}\rangle_\Omega.$$

The weak form of (3.9) is: Find $\boldsymbol{E} \in H(\mathrm{curl};\Omega)$ such that

$$B(\boldsymbol{w},\boldsymbol{E}) = 0, \quad \forall \boldsymbol{w} \in H(\mathrm{curl};\Omega). \tag{3.10}$$

To achieve a FE formulation the space $H(\mathrm{curl};\Omega)$ is replaced by a FE space

$$V^f = \left\{ \boldsymbol{v} \in H(\mathrm{curl};\Omega) : \boldsymbol{v} = \boldsymbol{a}^\ell H_\ell^{kmn},\ \ell \in \{u,v,w\},\ k,m,n \in \mathbb{Z}^+ \right\}.$$

Applying the FE space in the weak form, (3.10), leads to the matrix representation

$$[\mathbf{S}][\mathbf{b}] = k_0^2[\mathbf{M}][\mathbf{b}].$$

The elements of the matrices are

$$\begin{aligned}
[\mathbf{S}]_{e\ell'k'm'n'\ell kmn} =& \mu_\mathrm{c}^{-1}\langle \nabla\times\boldsymbol{a}^{\ell'}H_{\ell'}^{k'm'n'}, \nabla\times\boldsymbol{a}^{\ell}H_{\ell}^{kmn}\rangle_{\Omega_e},\\
[\mathbf{M}]_{e\ell'k'm'n'\ell kmn} =& \epsilon_\mathrm{c}\langle \boldsymbol{a}^{\ell'}H_{\ell'}^{k'm'n'}, \boldsymbol{a}^{\ell}H_{\ell}^{kmn}\rangle_{\Omega_e}
\end{aligned}$$

where $\ell',\ell \in \{u,v,w\}$ and Ω_e is the domain of cell e.

4 Results

The first example presented consists of the inhomogeneous waveguide including a rectangular dielectric inclusion. The width and height of the waveguide are $W = 0.11\,\mathrm{m}$ and $H = 0.1\,\mathrm{m}$, respectively, and the size of the inclusion is $w = 2.2\,\mathrm{cm}$ times $h = 2\,\mathrm{cm}$. The cross sectional surface has been divided into 25 identical cells, $N_x = 5$ and $N_z = 5$, where the inclusion represents the center cell. The frequency of operation is $f = 5\,\mathrm{GHz}$. The chosen eigenvalue corresponds to the fundamental mode for which the major part of the energy is concentrated around the inclusion. This can be seen in Figure 2 where the three components of the fundamental mode is illustrated for the case of $\epsilon_\mathrm{r} = 2$. To investigate the p-convergence, in the case of a real valued permittivity, the eigenvalue of the fundamental mode has been computed for nine different permittivity values at five different values of the order numbers of the polynomials of the basis functions. The maximum value of the order numbers has been chosen from the set $\{2,3,4,5,6\}$. The results are presented in Figure 3.

In the second example the influence of the complex valued permittivity on the p-convergence is studied. The eigenvalue has been computed for fourteen different conductivity values. The maximum value of the order numbers of the polynomials has been selected from the set $\{2,3,4,5,6\}$. The results are presented in Figure 4.

The reference values, that were produced by the FEM tool COMSOL, have an accuracy of six figures of merit. This states a lower bound of the accuracy which leads to the condition $|\gamma_N - \gamma| / |\gamma| > 10^{-6}$ where γ is the reference value of the

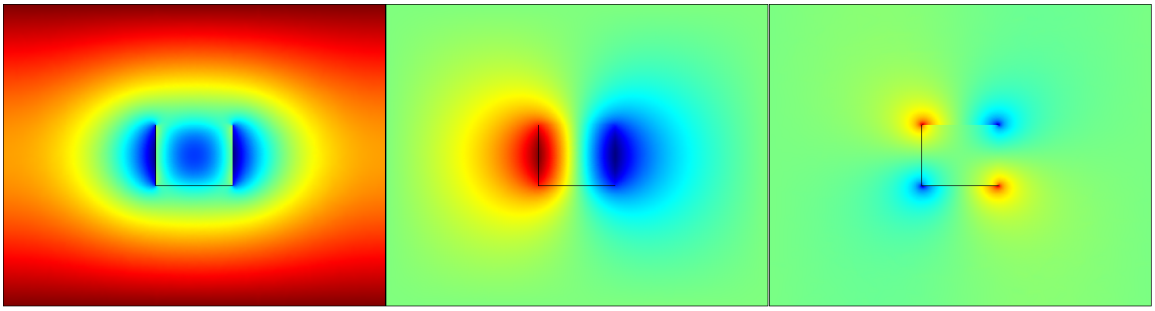

Figure 2: The three components of the mode corresponding to the TE_{01} mode of an empty waveguide. From left to right: $\mathrm{Re}(E_x)$, $\mathrm{Im}(E_y)$ and $\mathrm{Re}(E_z)$. The permittivity of the inclusion is $\epsilon_\mathrm{r} = 2$.

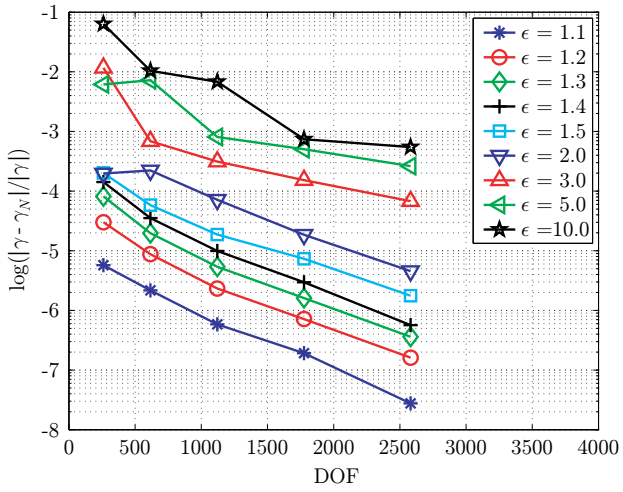

Figure 3: The relative error of the eigenvalue for the rectangular inhomogeneous waveguide.

eigenvalue and γ_N is the eigenvalue computed by the algorithm presented in this paper. This explains the behavior of the results in the left figure.

In the third, and last, example the p-convergence of the three lowest eigenvalues of the cubic homogeneous cavity is studied. In order to investigate the convergence the cavity is divided into a number of equally sized cubic cells to get the same number of cells in each direction, *i.e.*, $N_x = N_y = N_z$. The eigenvalues are thereafter computed for different order numbers of the polynomials. The maximum value of the order numbers, K, is chosen from the set $\{1, 2, 3, 4, 5, 6\}$. The results are presented in Figure 5. Due to limited RAM resources it has not been possible to study all combinations of K and N_x which means that the maximum value of K is not the same for all N_x.

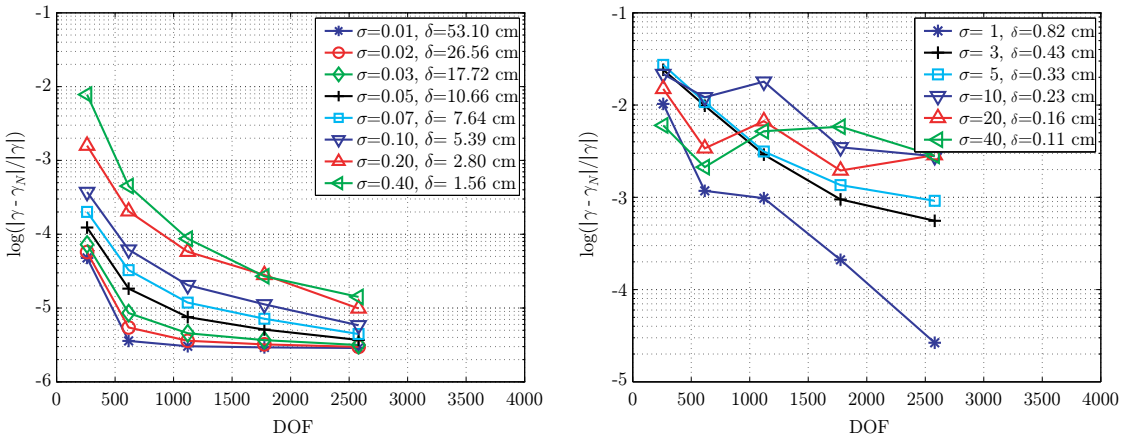

Figure 4: Relative error of the eigenvalues in the case of an inclusion of finite conductivity.

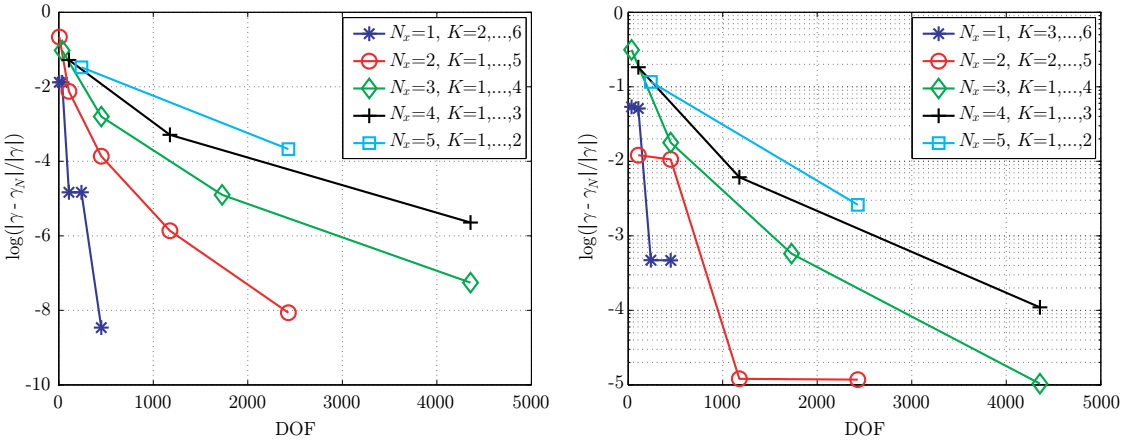

Figure 5: p-convergence for the cubic cavity for different number of cells. The left figure corresponds to the first and second eigenvalues and the right figure corresponds to the third eigenvalue.

5 Conclusions

The aim of this paper is to investigate the efficiency of the higher order hierarchical $H(\text{curl})$ Legendre basis functions in terms of p-convergence. Two different problems have been concerned: the inhomogeneous rectangular waveguide and the cubic homogeneous cavity. From the results of the first problem, in the case of a dielectric inclusion, we find that there exists a well defied p-convergence for all cases, *i.e.*, for $\epsilon_r \leq 10$ and that the convergence rate is approximately the same for the six cases between $\epsilon_r = 1.1$ and $\epsilon_r = 2$ (see Figure 3). Since this covers most of the realistic cases it seems like the basis functions are very efficient for this kind of problems, especially since the inclusion is spanned by one cell only. For the case of the conductive inclusion the p-convergence works very well for skin depth values that are

of the same size as the extension of the inclusion,
i.e., 2-2.2 cm (see Figure 4). It seems that the p-convergence is lost for skin depth values around $\delta = 0.2$ cm which corresponds to 10% of the extension of the inclusion. Thus the basis functions can be applied for this kind of problems as long as the size of the cells that spans the transmission line not exceeds the size of the skin depth.

The results from the second problem, as is presented in Figure 5, show that the basis functions are very efficient for three dimensional homogeneous problems. In the figure we notice that the shape of some off the lines is non smooth. The reason for the phenomenon is that basis functions that belong to the null space of the operator is added.

References

[1] G. E. Antilla and N. G. Alexopoulos. Scattering from complex three-domensional geometries by a curvilinear hybrid finite-element-integral equation approach. *J. Opt. Soc. Am. A*, **11**(4), 1445–1457, April 1994.

[2] A. Bossavit. Whitney forms: a class of finite elements for three-dimensional computations in electromagnetism. *IEE Proc. A*, **135**(8), 493–500, 1988.

[3] R. D. Graglia, D. R. Wilton, and A. F. Peterson. Higher order intepolatory vector bases for computational electromagnetics. *IEEE Trans. Antennas Propagat.*, **45**(3), 329–342, March 1997.

[4] P. Ingelström. Goal-oriented adaptivity using hierarchical basis functions on tetrahedral meshes. In *Third National Conference in Computational Electromagnetics, EMB04*, October 2004.

[5] E. Jørgensen, J. L. Volakis, P. Meincke, and O. Breinbjerg. Higher-order hierarchical Legendre basis functions for iterative integral equation solvers with curvilinear surface modeling. *Proc. IEEE Antennas Propagation Society Int. Symp.*, **4**, 618–621, June 2002.

[6] E. Jørgensen, J. L. Volakis, P. Meincke, and O. Breinbjerg. Higher Order Hierarchical Legendre Basis Functions for Electromagnetic Modeling. *IEEE Trans. Antennas Propagat.*, **52**(11), 2985–2995, November 2004.

[7] J. C. Nédélec. Mixed finite elements on r^3. *Numer. Math.*, **35**(3), 315–341, 1980.

[8] J. T. Oden and J. N. Reddy. *An Introduction to the Mathematical Theory of Finite Elements*. John Wiley & Sons, New York, 1973.

[9] J. A. Stratton. *Electromagnetic Theory*. McGraw-Hill, New York, 1941.

[10] M. G. Vanti and A. Raizer. Optimal Meshes and *h-p* Adaptivity. *IEEE Trans. Magnetics*, **33**(2), 1752–1755, March 1997.

[11] J. P. Webb. Hierarchal vector basis functins of arbitrary order for triangular and tetrahedral finite elements. *IEEE Trans. Antennas Propagat.*, **47**(8), 1244–1253, August 1999.